C−H versus Ir−X (X = H, Cl) Reactivity in a Tropylium PCP Pincer Iridium Complex[1]

Angelika M. Winter,[†] Klaus Eichele,[†] Hans-Georg Mack,[‡] William C. Kaska,*[,§] and Hermann A. Mayer*[,†]

Institut für Anorganische Chemie, Universität Tübingen, Auf der Morgenstelle 18, 72076 Tübingen, Germany, Institut für Physikalische und Theoretische Chemie, Universität Tübingen, Auf der Morgenstelle 8, 72076 Tübingen, Germany, and Department of Chemistry, University of California Santa Barbara, Santa Barbara, California 93106

Received September 12, 2004

The cationic tropylium $[(PCP')Ir(CO)(H)(Cl)]^+$ complex (**4**) (PCP′ = $[2,7\text{-}(CH_2P^tBu_2)_2C_7H_4]^+$) is generated from the neutral cycloheptatriene pincer complex (PCP)Ir(CO)(H)(Cl) (**1**) (PCP = $2,7\text{-}(CH_2P^tBu_2)_2C_7H_5$) by a hydride abstraction from the CH−Ir fragment with 1 equiv of trimethylsilyl trifluoromethanesulfonate. Interestingly, the tropylium ligand backbone in complex **4** is deprotonated by a base to give the neutral Ir(III) compound (PCP″)Ir(CO)(H)(Cl) (**5**) (PCP″ = $2\text{-}(CHP^tBu_2)\text{-}7\text{-}(CH_2P^tBu_2)C_7H_4$) with a π-system that extends into one of the phosphine bridges. Finally treatment of **5** with a further equivalent of a base removes HCl from the iridium center, forming the Ir(I) complex **6** with the same ligand backbone as in **5**. The HCl elimination and the deprotonation reactions are reversible. Thus addition of 2 equiv of HCl to **6** gives at first **5** then the tropylium complex **7**, which differs from **4** only by the counterion. The seven-membered aromatic tropylium system in **4** coordinates to the $Mo(CO)_3$ fragment, generating the bimetallic complex $[(CO)_3Mo(\eta^7\text{-}PCP')Ir(CO)(H)(Cl)]^+$ (**8**). Quantum chemical calculations at various levels of theory illustrated the relative energetic stabilities of all iridium complexes.

Introduction

Cyclic coordination of transition metals with anionic meridional, tridentate ligands has been studied since their first inceptions by Meek, van Koten, and Shaw.[2−7] The facile ability of these ligands to strongly coordinate a wide variety of transition and nontransition metals depends on the presence of at least two donor atoms and a C_{ipso}−metal bond to complement the structure. Molecular control of the bite angle, steric environment, and frontier orbitals can thereby be affected. Together these factors translate into materials with thermal stability, ease of coordination, and potential for interesting homogeneous catalysis.[7−13] Of particular importance is the presence of the one metal−carbon bond to enforce the structure. This prevents dissociation of the metal from the ligand under a variety of thermal conditions. In the meantime, thioether-based, nitrogen-based, oxygen-based, and phosphorus-based ligand systems have been developed.[8,9,14] Despite the broad scope of synthetic development that these ligands have undergone, the essential backbone has basically remained the same.[15−20]

This paper is devoted to the exploration of the cycloheptatrienyl moiety as the basic integral part of the pincer system in **1** (Scheme 1). The particular feature of the complexes described is their unsaturated but nonaromatic ligand backbone.[21] In particular a hydrogen atom is bound to the C_{ipso} atom. These features already became obvious in the first reactions described recently (Scheme 1).[21] By treatment with $LiBHEt_3$, a reagent typically employed to exchange a halide by a hydride ligand, a mixture of two unexpected products was obtained. The stable *trans*-dihydrido[22]

[†] Institut für Anorganische Chemie.
[‡] Institut für Physikalische und Theoretische Chemie.
[§] University of California Santa Barbara.

(1) This work is dedicated to Prof. Dr. E. Lindner on the occasion of his 70th birthday.
(2) Eller, P. G.; Bradley, D. C.; Hursthouse, M. B.; Meek, D. W. *Coord. Chem. Rev.* **1977**, *24*, 1.
(3) Alvarez, S. *Coord. Chem. Rev.* **1999**, *193−195*, 13.
(4) van Koten, G. *Pure Appl. Chem.* **1989**, *61*, 1681.
(5) Moulton, C. J.; Shaw, B. L. *J. Chem. Soc., Dalton Trans.* **1976**, 1020.
(6) van Koten, G.; Timmer, K.; Noltes, J. G.; Spek, A. L. *Chem. Commun.* **1978**, 250.
(7) Jensen, C. M. *Chem. Commun.* **1999**, 2443.
(8) Albrecht, M.; van Koten, G. *Angew. Chem., Int. Ed.* **2001**, *40*, 3750.
(9) Bergbreiter, D. E.; Osburn, P. L.; Liu, Y. S. *J. Am. Chem. Soc.* **1999**, *121*, 9531.
(10) Eberhard, M. R.; Wang, Z. *Org. Lett.* **2004**, *6*, 2125.
(11) Gu, X. Q.; Chen, W.; Morales-Morales, D.; Jensen, C. M. *J. Mol. Catal. A* **2002**, *189*, 119.
(12) van der Boom, M. E.; Milstein, D. *Chem. Rev.* **2003**, *103*, 1759.
(13) Goettker-Schnetmann, I.; Brookhart, M. *J. Am. Chem. Soc.* **2004**, *126*, 9330.
(14) Evans, D. R.; Huang, M.; Seganish, W. M.; Chege, E. W.; Lam, Y. F.; Fettinger, J. C.; Williams, T. L. *Inorg. Chem.* **2002**, *41*, 2633.
(15) Koridze, A. A.; Sheloumov, A. M.; Kuklin, S. A.; Lagunova, V. Y.; Petukhova, I. I.; Dolgushin, F. M.; Ezernitskaya, M. G.; Petrovskii, P. V.; Macharashvili, A. A.; Chedia, R. V. *Russ. Chem. Bull., Int. Ed.* **2002**, *51*, 1077.
(16) Nemeh, S.; Jensen, C.; Binamira-Soriaga, E.; Kaska, W. C. *Organometallics* **1983**, *2*, 1442.
(17) Farrington, E. J.; Martinez Viviente, E.; Williams, B. S.; van Koten, G.; Brown, J. M. *Chem. Commun.* **2002**, 308.
(18) Gossage, R. A.; McLennan, G. D.; Stobart, S. R. *Inorg. Chem.* **1996**, *35*, 1729.
(19) Fryzuk, M. D. *Can. J. Chem.* **1992**, *70*, 2839.
(20) Goettker-Schnetmann, I.; White, P. S.; Brookhart, M. *Organometallics* **2004**, *23*, 1766.
(21) Nemeh, S.; Flesher, R. J.; Gierling, K.; Maichle-Moessmer, C.; Mayer, H. A.; Kaska, W. C. *Organometallics* **1998**, *17*, 2003.

10.1021/om049289+ CCC: $30.25
Publication on Web 03/08/2005

Scheme 1

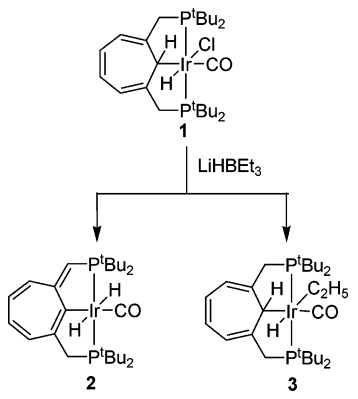

Scheme 2

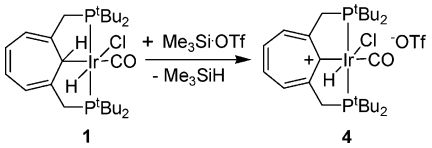

complex **2** is formed by removal of hydrogen chloride across the central metal−carbon bond and a consecutive hydrogen shift. Complex **2** thus clearly indicates the direct involvement of the ligand system in reactions of the cycloheptatrienyl pincer complex **1**. Even more unusual is the formation of the ethyl complex **3** by an untypical ligand exchange reaction of chloride by ethyl effected by "superhydride" $LiBHEt_3$. These few reactions already indicate the peculiar reactivity of cycloheptatrienyl pincer systems, which merit further investigation, to be described in the following.

Results and Discussion

Synthesis of the Tropylium PCP Pincer Triflate Complex 4. Treatment of the cycloheptatrienyl PCP pincer compound **1** with trimethylsilyl trifluoromethanesulfonate (Me_3SiOTf) gives the yellow tropylium triflate complex **4** in a clean reaction in almost quantitative yield (Scheme 2). The new tropylium system **4** is generated by abstraction of a hydride from the metal-bound ring carbon atom of **1**.[21] As the second product trimethylsilane is formed, which can easily be removed from the reaction mixture by evaporation. The described conversion has to be considered rather unusual, since the electrophile Me_3SiOTf is typically employed to replace a chlorine ligand by the less coordinating triflate anion in organometallic compounds.[23−25] The tropylium complex **4** dissolves well in polar solvents such as acetone, THF, and dichloromethane and is thermally stable (see below).

The structural assignment of **4** was confirmed by a number of spectroscopic techniques. In the $^{31}P\{^1H\}$ NMR spectrum of **4** the observed singlet at δ 63.4 is a result of a plane of symmetry perpendicular to the tropylium system which generates two chemically equivalent phosphine groups. Two sets of resonances each in the ^1H and $^{13}C\{^1H\}$ NMR spectra for the *tert*-butyl groups are thus a consequence of dissimilar *tert*-butyl groups at each of the *trans* ligands at the metal center. A triplet at δ −16.80 ($^2J_{PH}$ = 12.79 Hz) in the ^1H NMR spectrum confirms a hydride that is coordinated *trans* to a ligand with a weak *trans* influence like chlorine.[26] The positive charge of the ligand backbone is reflected in the ^1H and $^{13}C\{^1H\}$ NMR resonances of the seven-membered cycle. They experience a significant downfield shift as compared to **1**. The missing signals for the CH−Ir group in both spectra and a triplet at δ 213.3 ($^2J_{PC}$ = 3.03 Hz) in the $^{13}C\{^1H\}$ NMR spectrum are indicative of a positively charged carbon atom positioned at equal distance from the two phosphorus nuclei. The presence of the carbonyl ligand is established by a ν(C≡O) = 2030 cm^{-1} and a triplet in the ^{13}C NMR spectrum at δ 177.2 ($^2J_{PC}$ = 7.41 Hz).

As the chlorine could not be observed by mass spectrometry, an energy dispersive X-ray (EDX) spectrum was recorded.[27] The latter allows a fast and quantitative analysis of the elemental composition of a sample while requiring only minor amounts of substance. Thus it was confirmed by EDX that the molecular composition of **4** is in agreement with one chlorine atom per iridium atom as well as with the presence of a triflate anion. This is also reflected in the ^{19}F NMR spectrum, which displays a singlet at δ −76.9.

X-ray Single-Crystal Structure of the Tropylium Triflate 4. The structure of **4**, which was deduced by NMR spectroscopy in solution, was supported by an X-ray structure analysis in the solid state. A representation of the structure of **4** in the solid state is given in Figure 1; selected bond lengths and angles are collected in Table 1. Crystals of the PCP pincer tropylium triflate complex **4** were obtained by slow solvent evaporation from a solution of **4** in dichloromethane. Therefore, one molecule of solvent per molecule of **4** was found in the unit cell. The geometry around the iridium center is best described as a distorted octahedron with the phosphine groups bent away from the chlorine ligand. The two planes formed by the metal Ir(1), the carbon atoms C(11) and C(26), and one of the phosphorus atoms P(1) and P(2), respectively, enclose an angle of 165.8°. Due to the special geometry of the tropylium complex **4**, which incorporates two five-membered metallacycles, the phosphine groups are drawn back toward the tropylium ring, forming an P(1)−Ir(1)−P(2) angle of 160.8°. The presence of the chlorine ligand is obvious in the crystal structure. It is positioned *trans* to the hydride ligand, which could not be located but has been observed in the ^1H NMR spectrum. The seven-membered tropylium cycle of **4** is almost planar. This is due to the positively charged carbon atom whose empty p-orbital can overlap with the π-system of the ring. Thus an aromatic 6 π-electron arrangement delocalized over all seven ring carbon atoms is achieved. The C−C bond lengths in the cycle reflect this delocalization, with the longest distances at the metal-bound carbon atom (C(10)−C(11)

(22) Rybtchinski, B.; Ben-David, Y.; Milstein, D. *Organometallics* **1997**, *16*, 3786.
(23) Dani, P.; Toorneman, M. A. M.; van Klink, G. P. M.; van Koten, G. *Organometallics* **2000**, *19*, 5287.
(24) Conner, D.; Jayaprakash, K. N.; Cundari, T. R.; Gunnoe, T. B. *Organometallics* **2004**, *23*, 2724.
(25) Aizenberg, M.; Milstein, D. *J. Chem. Soc., Chem. Commun.* **1994**, 411.
(26) Mayer, H. A.; Kaska, W. C. *Chem. Ber.* **1995**, *128*, 95.
(27) Goldstein, J. I.; Newbury, D. E.; Echlin, P.; Joy, D. C.; Lyman, C. E.; Lifshin, E.; Sawyer, L.; Michael, J. R. In *Scanning Electron Microscopy and X-Ray Microanalysis*; Kluwer Academic/Plenum Publishers: New York, 2003; pp 297−536.

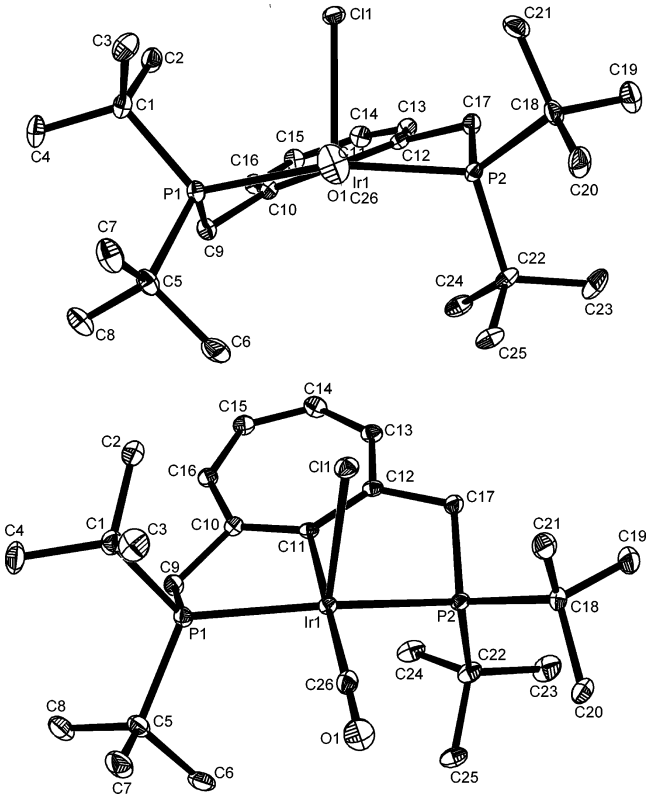

Figure 1. Different views of the molecular structure of **4** in the solid state (ORTEP plots). The triflate anion and hydrogen atoms have been omitted for clarity.

Table 1. Comparison of Selected Geometric Data of 4 from the X-ray Structure and DFT Calculations[a]

	experimental	SVWN/LACVP*	B3LYP/LACVP*
	Distances [Å]		
Ir(1)−P(1)	2.345(2)	2.334	2.402
Ir(1)−P(2)	2.342(2)	2.333	2.404
Ir(1)−C(11)	2.093(5)	2.065	2.107
Ir(1)−Cl(1)	2.496(2)	2.473	2.536
Ir(1)−C(26)	1.916(5)	1.895	1.927
O(1)−C(26)	1.128(7)	1.158	1.150
	Angles [deg]		
P(2)−Ir(1)−P(1)	160.8(1)	167.9	168.1
C(26)−Ir(1)−C(11)	179.7(2)	172.9	174.7
C(26)−Ir(1)−Cl(1)	95.9(2)	102.6	100.0
C(11)−Ir(1)−Cl(1)	83.9(2)	84.5	85.3
O(1)−C(26)−Ir(1)	177.4(5)	172.2	174.2

[a] For atom numbering see Figure 1.

1.427(7) Å and C(11)−C(12) 1.430(7) Å), which become shorter (minimum length C(14)−C(15) 1.368(8) Å) the further the bond is away from this carbon atom. This distribution of bond distances is in accordance with values obtained by density functional calculations (DFT, BLYP/6-31G*) of a cycloheptatrienylidene carbene fragment in the closed-shell singlet state ($^1A_1$) (Table 2).[28]

A particular feature of the tropylium complex **4** is the short C−O distance of the carbonyl ligand (1.128(7) Å). This is compatible with a strong CO bond, which is confirmed by IR spectroscopy. The ν(C≡O) band is shifted to higher wavenumbers by about 30 cm^{-1} as compared to **1**. This in turn is indicative of a weakened back-bonding from iridium into the antibonding π^*-orbital of the CO ligand. Therefore it can be concluded that the positive charge in the ring is delocalized even into iridium orbitals and thus reduces electron density which is necessary for Ir−CO back-bonding.

Table 2. Comparison of Bond Lengths [Å] of the Tropylium PCP Pincer Complex 4 with a Cycloheptatrienylidene Carbene Fragment (CHT)

	4[a]	CHT[b28]
C(11)−C(12)	1.430(7)	1.436
C(10)−C(11)	1.427(7)	
C(12)−C(13)	1.405(7)	1.411
C(10)−C(16)	1.402(7)	
C(13)−C(14)	1.380(8)	1.413
C(15)−C(16)	1.381(7)	
C(14)−C(15)	1.368(8)	1.398

[a] X-ray diffraction. [b] Density functional calculations (B3LYP/6-31G*).

Scheme 3

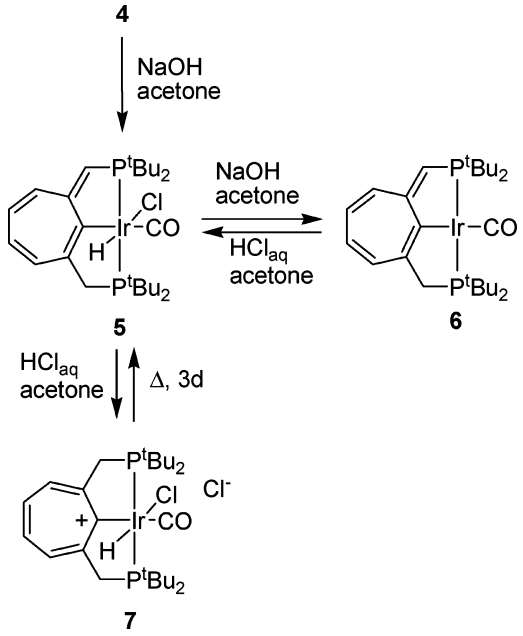

Reactivity of the Tropylium Triflate Complex 4. Complex **4** has been found to be stable toward an excess of air or water in the solid state and in solution, even upon reflux in acetone for 19 h. Upon treatment with an excess of nitrous oxide, no reaction can be observed, even after monitoring the reaction mixture by NMR spectroscopy for 16 days. In electrochemical experiments in dichloromethane between −2.0 and 1.6 V no oxidation or reduction peak could be observed.[29]

Reaction of 4 with Sodium Hydroxide. A remarkable sequence of reactions is observed when the cationic complex **4** is treated with an aqueous solution of sodium hydroxide (Scheme 3 and Figure 2). The sequence can be reversed by treatment of a solution of **6** with hydrogen chloride. Dropwise addition of a stoichiometric amount of an aqueous solution of sodium hydroxide to a solution of **4** in acetone results in a color change from orange to dark red after a reaction time of 3 h. Precipitation with *p*-xylene to remove byproducts gives the pure compound **5**. An AB pattern in the $^{31}P\{^1H\}$ NMR spectrum of the product **5** at δ 52.7 and 57.3 ($^2J_{PP}$ = 276.33 Hz) shows that a pronounced change in the

(28) Matzinger, S.; Bally, T.; Patterson, E. V.; McMahon, R. J. *J. Am. Chem. Soc.* **1996**, *118*, 1535.

(29) Speiser, B.; Novak, F. Personal communication.

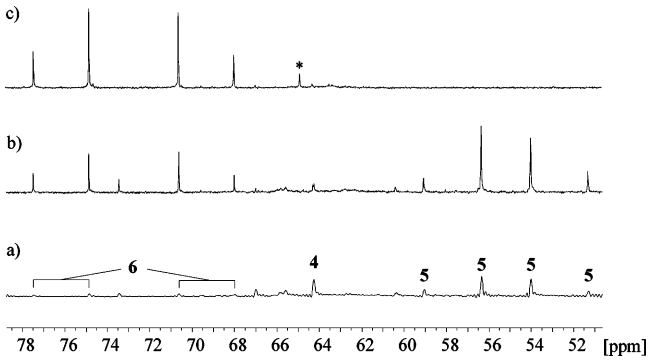

Figure 2. $^{31}P\{^1H\}$ NMR spectroscopic observation of the reaction of **4** with sodium hydroxide (a) immediately after addition; (b) after 7 days; (c) after a second addition of the reagent. *: impurities.

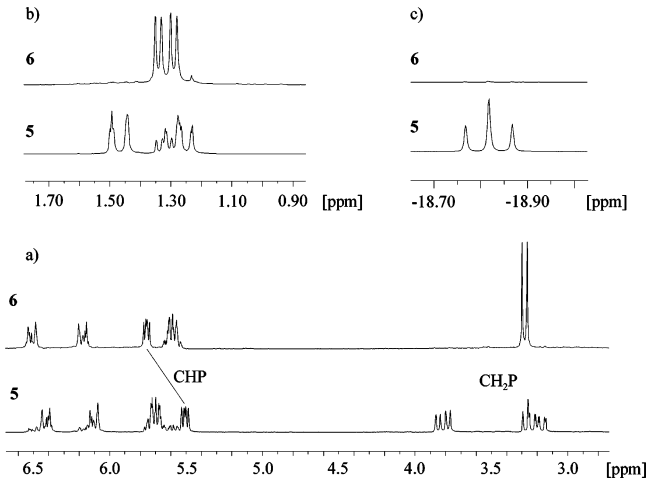

Figure 3. Comparison of ^1H NMR spectra of **5** and **6**: (a) CHP, CH_2P groups and ring protons; (b) tertiary butyl groups; (c) hydride region.

molecular structure of **4** has occurred. The most notable features in the ^1H NMR spectrum are two sets of resonances at δ 3.20 and 3.81, each being caused by only one proton (Figure 3a). They are due to one CH_2P group, as can be shown by H,H-COSY and C,H-correlation (HSQC) NMR experiments. A doublet of doublets at δ 5.50 ($^2J_{PH} = 6.91$ Hz, $^4J_{PH} = 4.08$ Hz, 1H) indicates that the bridge to the second phosphine group consists of a methine group. The base therefore abstracts a proton from one of the bridging methylene groups, which is followed by a rearrangement of the π-system in the cycloheptatriene backbone in a way that it is extended into one of the five-membered rings. Thus the neutral iridium(III) PCP pincer complex **5** is formed. The change within the ligand backbone is reflected not only in the signals of the bridging groups but naturally also in the ^1H NMR resonances of the ring protons. They are shifted to higher field by almost 3 ppm compared to **4**. Moreover due to the lower molecular symmetry of **5**, three instead of two signals are observed. A hydride multiplet (δ −18.86, dd, $^2J_{PH} = 12.56$ Hz, $^2J_{PH} = 12.56$ Hz) in the ^1H NMR spectrum confirms that no reaction has occurred directly at the metal center (Figure 3c). The $^{13}C\{^1H\}$ NMR spectrum is in agreement with the assignment of the solution structure of **5**. It contains one doublet at δ 43.0 ($^1J_{PC} = 24.93$ Hz), which a DEPT135 experiment confirms to be caused by the CH_2P group. In addition to the four resonances of the CH groups of the cycloheptatrienyl moiety, a fifth CH signal at δ 114.7 (dd, $^1J_{PC} = 46.48$ Hz, $^3J_{PC} = 4.72$ Hz) is caused by the CHP group. As a result of the neutral cycloheptatrienyl cycle, the resonance of the iridium-coordinated ring carbon atom at δ 132.2 is dramatically shifted to higher field in comparison to **4**. Sodium triflate, which forms in the reaction of PCP pincer tropylium triflate **4** with sodium hydroxide, can easily be removed by precipitation with xylene. Again the infrared carbonyl stretching frequency is a good probe to observe the changes in the ligand system. A band at 2000 cm^{-1} for **5** corresponds to a shift by 30 cm^{-1} to lower wavenumbers in comparison to **4**, which indicates a weakened CO bond. Therefore the π-acidity of the cycloheptatrienyl π-system is reduced in **5**.

The cycloheptatrienyl PCP pincer iridium(III) complex **5** continues to react with sodium hydroxide (Scheme 3 and Figure 2). With a stoichiometric amount of the reagent a dark red solution forms at ambient temperature, and after purification with pentane the iridium(I) complex **6** is isolated. Interestingly this is a rare example of a base-induced reduction of an iridium(III) compound to an iridium(I) complex. As this reaction proceeds rather easily, compound **5** is usually contaminated with traces of **6** in the reaction of **4** with sodium hydroxide.

Due to the identical ligand backbone, the differences in the NMR spectra of complexes **5** and **6** (Figure 3) are caused by the different metal oxidation state and the molecular symmetry. In the $^{31}P\{^1H\}$ NMR spectrum of **6** the AB pattern (δ 69.0 and 75.3, $^2J_{PP} = 266.56$ Hz) is shifted downfield compared to the Ir(III) complex **5**. No hydride signal is observed in the ^1H NMR spectrum of **6**, and the two protons on the CH_2P group give rise to only one doublet at δ 3.28 ($^2J_{PH} = 8.22$ Hz). The $^{13}C\{^1H\}$ NMR spectrum of **6** again is similar to **5** and confirms that the most distinct change has occurred at the metal center. A pronounced downfield shift is observed for both iridium-coordinated carbon atoms of 19 ppm (CO) and 62 ppm (IrC), respectively. The carbonyl stretching frequency in the infrared spectrum of **6** at 1919 cm^{-1} is again shifted to smaller wavenumbers, indicating that the back-bonding from iridium to the carbonyl group is increased by the reduction of iridium.

To investigate whether the formation reaction of **6** from **5** is reversible, the iridium(I) PCP pincer complex **6** was treated both with hydrochloric acid as well as with gaseous hydrogen chloride. In the first case, the red solution of **6** in acetone immediately turns orange when hydrochloric acid is added. After the reaction is terminated by evaporation of the solvent, according to ^1H and $^{31}P\{^1H\}$ NMR spectroscopy a mixture of two products is obtained that contains **5** in 53.4% and the tropylium chloride complex **7** in 46.6% yield. When **6** is treated with gaseous hydrogen chloride, the immediate formation of the cationic complex **7** is indicated by a color change from red to yellow. A comparison of the two reactions described shows that in agreement with the principle of microscopic reversibility the reaction of the tropylium PCP pincer complex **4** with a base yields **6** via **5**. Treatment of **6** with an acid reverses the sequence

by first giving **5** and in a second step forming the tropylium chloride **7**. The structural identification of **7** is achieved by comparison of the NMR spectra of both tropylium compounds **4** and **7**. They are virtually similar in chemical shifts, multiplicities, and coupling constants of all resonances except for minor variations resulting from the different counterions. A ^{19}F NMR spectrum of **7** displays no signal since triflate is no longer available as anion. The presence of chloride as the anionic part of the structure, as expected on the grounds of the reaction performed, was again confirmed by EDX spectroscopy. The reduced chlorine content observed in the EDX spectrum of **7** is due to HCl elimination under the experimental conditions in the scanning electron microscope. This ease of hydrogen chloride loss can be confirmed experimentally. When heating the dry tropylium chloride complex **7** under vacuum, the yellow color changes to red after 3 days and a white solid sublimes. $^{31}P\{^1H\}$ NMR spectroscopic observation of the reaction indicates that after this period of time an equilibrium has been reached consisting of 66.4% of **5** and 33.6% of **7**.

Scheme 4

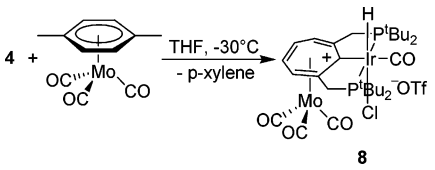

8

Treatment of 4 with (η^6-*p*-xylene)Mo(CO)$_3$. Following the reaction procedure described by Tamm and co-workers[30] an attempt was made to coordinate the molybdenum tricarbonyl moiety to the tropylium ring of **4** as a second metal fragment. By treating the PCP pincer tropylium complex **4** in THF with (η^6-*p*-xylene)-Mo(CO)$_3$ the orange-brown bimetallic complex **8** is obtained after 30 min (Scheme 4). At −30 °C the yield is 85%, whereas at room temperature only 70% of **8** is obtained. Further workup of the reaction mixture proved to be difficult since complex **8** readily decomposes in solution. This is assumed to be caused by impurities resulting from the decomposition of the molybdenum starting material in the THF solution.[31] The coordination of a second metal fragment to **4** can be confirmed spectroscopically. Because the major structural change in **8** has occurred at the seven-membered ring, the number of resonances in the NMR spectra remain almost unchanged in comparison to **4**. Thus the $^{31}P\{^1H\}$ NMR spectrum of **8** displays a singlet at δ 48.3. The ^1H and $^{13}C\{^1H\}$ NMR resonances of the ring are significantly shifted to higher field as compared to the tropylium triflate **4**. The most dramatic change is observed for the metal-bound ring carbon atom. Its resonance is moved to higher field by 84 ppm. The coordination of a molybdenum tricarbonyl moiety to **4** is most distinctly mirrored in the infrared spectrum. Four ν(CO) vibrations are observed at 2045, 2030, 1981, and 1940 cm^{-1} for the carbonyl ligands at iridium and molybdenum. These bands are distinctly shifted compared to the starting material (η^6-*p*-xylene)Mo(CO)$_3$ with ν(CO) at 1963 and 1883 cm^{-1}. Upon ionization by fast atom bombardment (FAB), the cationic part of **8** can even be detected by mass spectrometry.

Table 3. Relative Thermodynamical Stabilities [kcal/mol] of the Complexes Discussed

complex	SVWN/LACVP*	B3LYP/LACVP*
1	0.0	0.0
4′/7′	219.8	203.3
5	30.0	16.2
6	74.1	37.7
8′	138.5	155.1

Quantum Chemical Calculations. The unusual ligand reactivity of the PCP pincer tropylium triflate complex prompted us to perform DFT calculations at various levels of theory. All tertiary butyl groups were included in the calculations, since they have been found to play an important role in the reactivity of pincer complexes.[16,24,32,33] For the charged complexes **4**, **7**, and **8** the anion has been omitted in the calculations (marked by primes). For further computational details see the Experimental Section.

The relative energetic stabilities of the compounds are presented in Table 3. The cycloheptatrienyl PCP pincer complex **1** is predicted by both computational procedures (SVWN/LACVP*, B3LYP/LACVP*) to be the most stable one. The SVWN approach in most cases yields somewhat higher energies even though the relative energy differences are similar in both cases. For the charged complexes a much higher energy is obtained than for the neutral ones. Since all calculations have been carried out for gas-phase molecules, solvent effects, which certainly play a considerable role for the cationic species, have not been considered. This explains why the tropylium triflate **4** has been found to be very stable in experiments, although the calculations predict a low thermodynamical stability. However, a comparison of the cationic complexes **4′**, **7′**, and **8′** still is possible. Complexes **4′** and **7′** are of the same energy, since they only differ in the anion, which has not been considered in the calculations. A comparison of the bimetallic complex **8′** with **4′** demonstrates that a pronounced stabilization of 48.2 kcal/mol (B3LYP/LACVP*) has been achieved by the coordination of a second metal fragment. Complexes **5** and **6** are somewhat destabilized in comparison to **1**, with **5** being lower in energy by 21.5 kcal/mol (B3LYP/LACVP*) compared to **6**.

For the tropylium complex **4** a comparison of the geometric data obtained by quantum chemical calculations with those found by X-ray single-crystal analysis reveals a good match (Table 1). The results obtained by using the B3LYP functional mirror the experimental values somewhat better than the SVWN results. The large deviation of the calculated C−O bond length from the X-ray structural data is due to the fact that multiple bonds are generally underestimated in X-ray structural analysis. The rather big differences between the experimental and calculated P−Ir−P and C−Ir−C angles are certainly due to packing effects originating from intermolecular interactions in the solid state. Since equilib-

(30) Tamm, M.; Bannenberg, T.; Dressel, B. *Organometallics* **2001**, *20*, 900.

(31) Hoff, C. D. *J. Organomet. Chem.* **1985**, *282*, 201.

(32) Mohammad, H. A. Y.; Grimm, J. C.; Eichele, K.; Mack, H. G.; Speiser, B.; Novak, F.; Quintanilla, M. G.; Kaska, W. C.; Mayer, H. A. *Organometallics* **2002**, *21*, 5775.

(33) van der Boom, M. E.; Iron, M. A.; Atasoylu, O.; Shimon, L. J. W.; Rozenberg, H.; Ben David, Y.; Konstantinovski, L.; Martin, J. M. L.; Milstein, D. *Inorg. Chim. Acta* **2004**, *357*, 1854.

rium structures resulting from quantum chemical calculations refer to gas-phase molecules at 0 K, a comparison to gas-phase electron diffraction results is much better suited.

This agreement of theoretically obtained and experimental complex geometry allows to consider the calculated structures of **5**, **6**, and **8**, where no experimental structural data are available. The geometry of both cycloheptatrienyl PCP pincer complexes **5** and **6** is very similar. The distribution of bond lengths in the ligand backbone closely mirrors the bonding pattern of the cycloheptatrienyl structure with the π-system extending into one of the bridges to the phosphine groups. The seven-membered cycle is almost planar in both cases, being slightly bent at the carbon atoms bearing the bridges. A slight tilt of the ring toward the ligand square around the metal is observed. The central metal is either in an octahedral (as in **5**) or a planar (as in **6**) coordination geometry with a P−Ir−P angle in the range 163−165°.

In the case of the bimetallic complex **8**, the effect of the coordination of the molybdenum tricarbonyl fragment is clearly discernible in the structural data derived from quantum chemical calculations. The ligand geometry around iridium is virtually unaffected by the coordination of the molybdenum fragment. The only differences observed between **8** and **4** are directly at the seven-membered ring. The cycle of **8** is absolutely planar. The almost equal length of all C−C bonds in the ring, covering a range of 1.400−1.452 Å, reflects the charge delocalization within the aromatic system. As can be expected, these bonds are elongated by the coordination of the $Mo(CO)_3$ fragment in comparison to **4**, where the C−C bond distances lie in the range 1.368−1.430 Å. The calculations additionally indicate that neither of the two sides of the seven-membered ring is favored in the addition of molybdenum tricarbonyl. The SVWN functional predicts a higher stability for a coordination on the side of the iridium-bound hydride ligand by 4.3 kcal/mol, whereas the B3LYP calculations yield a higher stability of 2.9 kcal/mol for a coordination on the side of the chloride substituent.

Conclusion

The behavior of trimethylsilyltriflate as a strong electrophile seems unusual. Despite the extreme affinity of silicon for chlorine, it leaves the metal-bound chlorine ligand in **1** untouched and eliminates a hydride from the CH−Ir fragment in the cycloheptatriene ring. Thus the product tropylium triflate complex **4** incorporates a cationic seven-membered ring in which the positive charge is delocalized over all seven carbon atoms and even extends into metal-based orbitals. Furthermore as a consequence of the positive charge of the ligand backbone, the hydrogen atoms on the methylene bridges to the phosphine groups become acidic. A base easily removes a proton from one of the CH_2 bridges, yielding the neutral cycloheptatrienyl pincer complex **5** with an extended π-system. In total the two reactions dehydrogenate the ligand backbone. The aromatic six-electron π-system is considered as the driving force of the observed hydride elimination. In addition the formation of a stable Ir−C(sp^2) bond in **4** and **5** also favors a reaction at the ligand backbone over an attack at the Ir−H bond. Hoff and Bergman have noted that the bond of iridium to an sp^2-hybridized carbon atom is considerably more stable than an Ir−C(sp^3) bond.[34]

Complex **5** is predicted by quantum chemical calculations to be rather stable. This stability is also reflected in the ease of formation of **5** from various complexes. However, with 1 equiv of base it easily can be converted to the iridium(I) complex **6**. This confirms that once the ligand is deactivated, the base consequently attacks the metal center at the Ir−H bond. By reaction with an acid, **6** in turn can be converted back to the tropylium system **7** via **5**. This ease of interconversion between several complexes of different ligand structure or metal oxidation state is a particular feature of the seven-membered pincer systems. The reactions discussed demonstrate that by variations in the ligand backbone the complex reactivity can be directed to either C−H groups within the backbone or the metal center itself. Although quantum chemical calculations predict a difference in thermodynamical stabilities of the complexes **4′/7′**, **5**, and **6**, the experimentally observed ease of interconversion indicates the particularity of the pincer structure under consideration.

Experimental Section

All operations were carried out under argon using standard Schlenk techniques.[35] Toluene and *p*-xylene were distilled from sodium benzophenone ketyl, acetone from potassium carbonate, and pentane from lithium aluminum hydride. Trimethylsilyl trifluoromethanesulfonate was purchased from Fluka Chemical Company and vacuum distilled prior to use. The 0.1 N hydrochloric acid was purchased from Merck Chemical Company. All deuterated solvents as well as the acid and base were degassed three times before use applying the freeze−pump−thaw methodology and stored under argon. Compound **1** was synthesized following literature procedures.[21]

Synthesis of 4. Trimethylsilyl trifluoromethanesulfonate (86 μL, 0.475 mmol) is added quickly to 0.302 g (0.445 mmol) of **1** in 10 mL of toluene. The mixture is reacted for 1 h, after which all volatiles are removed in vacuo, yielding a dark orange solid. Complex **4** is obtained as a yellow solid by precipitation with acetone/pentane. Slow evaporation of dichloromethane yields crystals suitable for X-ray diffraction. Yield: 0.369 g (0.454 mmol; 99.8%). ^{1}H NMR (250.13 MHz, acetone-d_6): δ −16.80 (t, $^2J_{PH}$ = 12.79 Hz, 1H, IrH), 1.36 ($A_9XX'A_9'$, N = $|^3J_{PH} + {}^5J_{PH}|$ = 14.25 Hz, 18H, $C(CH_3)_3$), 1.51 ($A_9XX'A_9'$, N = $|^3J_{PH} + {}^5J_{PH}|$ = 15.09 Hz, 18H, $C(CH_3)_3$), 4.67 ($[ABX]_2$, $J_{AB} = {}^2J_{HH}$ = 17.18 Hz, N = $|^2J_{PH} + {}^4J_{PH}|$ = 7.76 Hz, 2H, CH_aH_bP), 4.96 ($[ABX]_2$, $J_{AB} = {}^2J_{HH}$ = 17.18 Hz, N = $|^2J_{PH} + {}^4J_{PH}|$ = 6.94 Hz, 2H, CH_aH_bP), 8.54 ($[AB]_2$, N = $|^3J_{HH} + {}^4J_{HH}|$ = 22.22 Hz, 2H, =CH), 8.95 ($[AB]_2$, N = $|^3J_{HH} + {}^4J_{HH}|$ = 22.22 Hz, 2H, =CH). ^{31}P{^{1}H} NMR (101.26 MHz, acetone-d_6): δ 63.4 (s). ^{19}F NMR (235.33 MHz, acetone-d_6): δ −76.9 (s). ^{13}C{^{1}H} NMR (62.90 MHz, acetone-d_6): δ 29.5 (m, $C(CH_3)_3$), 30.1 (m, $C(CH_3)_3$), 37.7 (AXX′, N = $|^1J_{PC} + {}^3J_{PC}|$ = 26.95 Hz, $C(CH_3)_3$), 39.7 (AXX′, N = $|^1J_{PC} + {}^3J_{PC}|$ = 21.56 Hz, $C(CH_3)_3$), 47.6 ($[AX]_2$, N = $|^1J_{PC} + {}^3J_{PC}|$ = 27.62 Hz, CH_2P), 128.5 (q, $^1J_{CF}$ = 50.33 Hz, CF_3), 143.7 ($[AX]_2$, N = $|^3J_{PC} + {}^4J_{PC}| + |^4J_{PC} + {}^5J_{PC}|$ = 12.80 Hz, =CH), 146.9 (s, =CH), 177.2 (t, $^2J_{PC}$ = 7.41 Hz, CO), 179.8 ($[AX]_2$, N = $|^2J_{PC} + {}^3J_{PC}| + |^3J_{PC} + {}^4J_{PC}|$ = 13.47 Hz, $CHCCH_2P$), 213.3 (t, $^2J_{PC}$ = 3.03 Hz, C^+). IR (cm^{-1}, pellet on KBr): 2030 (vs) ν(C=O). MS (FD): *m/z* 626.5 [M^+ − (HCl +

(34) Stoutland, P. O.; Bergman, R. G.; Nolan, S. P.; Hoff, C. D. *Polyhedron* **1988**, *7*, 1429.

(35) Wayda, A. L., Darensbourg, M. Y., Eds. *Experimental Organometallic Chemistry. A Practicum in Synthesis and Characterization*; ACS Symposium Series 357; 1987; p 299.

$OS(O)_2CF_3$)], calcd for $C_{26}H_{44}OP_2Ir$: 626.8. Elemental Analysis: Anal. Calcd for $C_{27}H_{45}P_2O_4SF_3ClIr$: C: 39.92; H: 5.58; S: 3.95. Found: C: 40.61; H: 5.73; S: 3.55. EDX (weight fraction): Anal. Calcd for $C_{27}P_2O_4SF_3ClIr$: C: 42.3; P: 8.1; O: 8.3; S: 4.2; Cl: 4.6; Ir: 25.1. Found: C: 44.9; P: 7.6; O: 7.8; S: 4.4; Cl: 4.6; Ir: 27.0; these were repeat analyses.

Synthesis of 5. Method A. To a solution of **4** (0.062 g, 0.076 mmol) in 6 mL of acetone is added dropwise a freshly prepared aqueous solution of sodium hydroxide (80 μL, 0.079 mmol, 0.99 N). The reaction mixture is stirred for 3 h at ambient temperature, after which a change of color from orange to dark red occurs. All volatiles are removed, the residue is dissolved in *p*-xylene and filtered, and the product complex **5** is isolated as a red solid by drying of the filtrate. Yield: 0.041 g (0.063 mmol, 82.9%).

Method B. Hydrochloric acid (0.2 mL, 0.020 mmol, 0.1 N) is added dropwise to 0.034 g (0.054 mmol) of **6** in 3 mL of acetone. The reaction mixture immediately turns orange, and the reaction is stopped by evaporating the solvent. A mixture of complexes **5** (53.35% according to ^{1}H and ^{31}P{^{1}H} NMR spectroscopy) and **7** (46.65%) is obtained.

Method C. Under vacuum 0.044 g (0.063 mmol) of **7** is heated at 60−110 °C for 3 days, after which the yellow solid turns red and a white solid sublimes. The equilibrium mixture contains **5** (66.4% according to ^{31}P{^{1}H} NMR spectroscopy) and **7** (33.6%). ^{1}H NMR (250.13 MHz, $CDCl_3$): δ −18.86 (dd, $^2J_{PH}$ = 12.56 Hz, 12.56 Hz, 1H, IrH), 1.27 (m, 18H, C(CH_3)$_3$), 1.46 (m, 18H, C(CH_3)$_3$), 3.20 (ddd, $^2J_{HH}$ = 16.13 Hz, $^2J_{PH}$ = 10.28 Hz, $^4J_{PH}$ = 2.12 Hz, 1H, CH_aH$_b$P), 3.81 (dd, $^2J_{HH}$ = 16.13 Hz, $^2J_{PH}$ = 7.22 Hz, 1H, CH$_a$$H_b$P), 5.50 (dd, $^2J_{PH}$ = 6.91 Hz, $^4J_{PH}$ = 4.08 Hz, 1H, CHP), 5.69 (m, 2H, =CH), 6.10 (m, 1H, =CH), 6.41 (m, 1H, =CH). ^{31}P{^{1}H} NMR (101.26 MHz, $CDCl_3$): δ 52.7 (d, AB, $^2J_{PP}$ = 276.33 Hz), 57.3 (d, AB, $^2J_{PP}$ = 276.33 Hz). ^{13}C{^{1}H} NMR (62.90 MHz, $CDCl_3$): δ 29.6 (m, C(*C*H$_3$)$_3$), 30.3 (m, C(*C*H$_3$)$_3$), 31.2 (m, C(*C*H$_3$)$_3$), 36.1 (dd, $^1J_{PC}$ = 27.28 Hz, $^3J_{PC}$ = 3.71 Hz, *C*(CH$_3$)$_3$), 36.8 (dd, $^1J_{PC}$ = 23.58 Hz, $^3J_{PC}$ = 4.04 Hz, *C*(CH$_3$)$_3$), 37.8 (dd, $^1J_{PC}$ = 14.82 Hz, $^3J_{PC}$ = 5.39 Hz, *C*(CH$_3$)$_3$), 39.2 (dd, $^1J_{PC}$ = 18.86 Hz, $^3J_{PC}$ = 6.74 Hz, *C*(CH$_3$)$_3$), 43.0 (d, $^1J_{PC}$ = 24.93 Hz, CH$_2$P), 114.7 (dd, $^1J_{PC}$ = 46.48 Hz, $^3J_{PC}$ = 4.72 Hz, CHP), 126.6 (d, $^4J_{PC}$ = 1.35 Hz, =CH), 128.0 (s, =CH), 132.0 (d, $^3J_{PC}$ = 20.21 Hz, =CH), 132.1 (d, $^3J_{PC}$ = 19.54 Hz, =CH), 132.2 (s, IrC), 146.2 (dd, $^2J_{PC}$ = 10.11 Hz, $^4J_{PC}$ = 3.37 Hz, CH*C*CP), 171.2 (dd, $^2J_{PC}$ = 20.21 Hz, $^4J_{PC}$ = 4.04 Hz, CH*C*CP), 178.2 (dd, $^2J_{PC}$ = 6.74 Hz, 6.74 Hz, CO). IR (cm^{-1}, pellet on KBr): 2000 (vs) ν(C=O). MS (FD): *m/z* 661.2 [M$^+$ − H], calcd for $C_{26}H_{43}ClOP_2Ir$: 661.2; 627.2 [M$^+$ − Cl], calcd for $C_{26}H_{44}OP_2Ir$: 626.8. EDX (weight fraction): Anal. Calcd for $C_{26}ClOP_2Ir$: C: 50.5; Cl: 5.7; O: 2.6; P: 10.0; Ir: 31.1. Found: C: 49.5; Cl: 6.3; O: 7.2; P: 9.9; Ir: 27.2.

Synthesis of 6. Method A. Complex **5** (0.016 g, 0.024 mmol) is dissolved in 2.5 mL of acetone and treated with 50 μL (0.024 mmol, 0.5 N) of an aqueous solution of sodium hydroxide for 1.5 h at ambient temperature. The resulting dark red solution is dried, and the product is dissolved in pentane and filtered. **6** is obtained as a red solid by evaporation of the filtrate. Yield: 0.008 g (0.013 mmol, 43.3%).

Method B. Reaction Monitoring. 4 (0.011 g, 0.014 mmol) in 0.5 mL of acetone-d_6 is treated with 20 μL (0.019 mmol, 0.96 N) of a freshly prepared aqueous solution of sodium hydroxide. After 8 days another 32 μL (0.014 mmol, 0.425 N) of sodium hydroxide in water is added. The progress of the reaction is monitored by ^{31}P{^{1}H} NMR spectroscopy. ^{1}H NMR (250.13 MHz, $CDCl_3$): δ 1.31 (d, $^3J_{PH}$ = 13.02 Hz, 18H, C(CH_3)$_3$), 1.33 (d, $^3J_{PH}$ = 12.56 Hz, 18H, C(CH_3)$_3$), 3.28 (d, $^2J_{PH}$ = 8.22 Hz, 2H, CH_2P), 5.59 (m, 2H, =CH), 5.76 (dd, $^2J_{PH}$ = 5.71 Hz, $^4J_{PH}$ = 3.65 Hz, 1H, CHP), 6.17 (m, 1H, =CH), 6.51 (m, 1H, =CH). ^{31}P{^{1}H} NMR (101.26 MHz, $CDCl_3$): δ 69.0 (d, AB, $^2J_{PP}$ = 266.56 Hz), 75.3 (d, AB, $^2J_{PP}$ = 266.56 Hz). ^{13}C{^{1}H} NMR (62.90 MHz, $CDCl_3$): δ 29.8 (dd, $^2J_{PC}$ = 4.04 Hz, $^4J_{PC}$ = 0.34 Hz, C(*C*H$_3$)$_3$), 30.0 (dd, $^2J_{PC}$ = 4.38 Hz, $^4J_{PC}$ = 0.34 Hz, C(*C*H$_3$)$_3$), 36.1 (dd, $^1J_{PC}$ = 20.55 Hz, $^3J_{PC}$ = 2.69 Hz, *C*(CH$_3$)$_3$), 36.6 (dd, $^1J_{PC}$ = 24.42 Hz, $^3J_{PC}$ = 2.86 Hz, *C*(CH$_3$)$_3$), 45.5 (dd, $^1J_{PC}$ = 26.27 Hz, $^3J_{PC}$ = 1.01 Hz, CH_2P), 119.3 (dd, $^1J_{PC}$ = 45.98 Hz, $^3J_{PC}$ = 1.85 Hz, CHP), 126.5 (d, $^4J_{PC}$ = 1.35 Hz, =CH), 127.7 (s, =CH), 131.4 (d, $^3J_{PC}$ = 16.17 Hz, =CH), 133.5 (d, $^3J_{PC}$ = 21.22 Hz, =CH), 152.7 (dd, $^2J_{PC}$ = 15.49 Hz, $^4J_{PC}$ = 4.76 Hz, CH*C*CP), 172.7 (dd, $^2J_{PC}$ = 24.59 Hz, $^4J_{PC}$ = 4.72 Hz, CH*C*CP), 194.0 (dd, $^3J_{PC}$ = 3.54 Hz, $^3J_{PC}$ = 2.53 Hz, IrC), 196.5 (dd, $^2J_{PC}$ = 8.42 Hz, 8.42 Hz, CO). IR (cm^{-1}, pellet on KBr): 1919 (vs) ν(C=O). MS (FD): *m/z* 626.7 [M$^+$], calcd for $C_{26}H_{43}OP_2Ir$: 625.8. EDX (weight fraction): Anal. Calcd for $C_{26}OP_2Ir$: C: 53.6; O: 2.7; P: 10.6; Ir: 33.0; Found: C: 51.7; O: 6.1; P: 12.3; Ir: 27.4; Cl: 2.5.

Synthesis of 7. Complex **6** (0.008 g, 0.013 mmol) in 5 mL of acetone is treated with gaseous hydrogen chloride made from ammonium chloride and concentrated sulfuric acid. An immediate change in color from red to yellow indicates the completion of the reaction. The solvent is evaporated, yielding **7** as a yellow solid. The same product is obtained when starting from a mixture of complexes **5** and **6**. Yield: 0.009 g (0.013 mmol, quantitative). ^{1}H NMR (250.13 MHz, $CDCl_3$): δ −17.26 (t, $^2J_{PH}$ = 12.56 Hz, 1H, IrH), 1.27 ($A_9XX'A_9'$, N = |$^3J_{PH}$ + $^5J_{PH}$| = 14.16 Hz, 18H, C(CH_3)$_3$), 1.46 ($A_9XX'A_9'$, N = |$^3J_{PH}$ + $^5J_{PH}$| = 15.08 Hz, 18H, C(CH_3)$_3$), 4.36 (d, AB, br, $^2J_{HH}$ = 16.90 Hz, 2H, CH_aH$_b$P), 4.91 (d, AB, br, $^2J_{HH}$ = 16.90 Hz, 2H, CH$_a$$H_b$P), 8.46 (s, br, 2H, =CH), 9.10 (s, br, 2H, =CH). ^{31}P{^{1}H} NMR (101.26 MHz, $CDCl_3$): δ 63.4 (s). ^{13}C{^{1}H} NMR (62.90 MHz, CD_2Cl_2): δ 30.0 (m, C(*C*H$_3$)$_3$), 37.4 (AXX′, N = |$^1J_{PC}$ + $^3J_{PC}$| = 26.27 Hz, *C*(CH$_3$)$_3$), 39.4 (AXX′, N = |$^1J_{PC}$ + $^3J_{PC}$| = 20.88 Hz, *C*(CH$_3$)$_3$), 47.6 ([AX]$_2$, N = |$^1J_{PC}$ + $^3J_{PC}$| = 26.94 Hz, CH_2P), 143.1 ([AX]$_2$, N = |$^3J_{PC}$ + $^4J_{PC}$| + |$^4J_{PC}$ + $^5J_{PC}$| = 12.80 Hz, =CH), 146.5 (s, =CH), 175.8 (t, $^2J_{PC}$ = 7.41 Hz, CO), 178.4 ([AX]$_2$, N = |$^2J_{PC}$ + $^3J_{PC}$| + |$^3J_{PC}$ + $^4J_{PC}$| = 13.48 Hz, CH*C*CH$_2$P), 213.0 (t, $^2J_{PC}$ = 4.38 Hz, C$^+$). IR (cm^{-1}, pellet on KBr): 2024 (vs) ν(C=O). MS (FAB): *m/z* 661.2 [M$^+$ − (H + HCl)], calcd for $C_{26}H_{43}ClOP_2Ir$: 661.2; 627.2 [M$^+$ − (HCl + Cl)], calcd for $C_{26}H_{44}OP_2Ir$: 626.8. EDX: (weight fraction): Anal. Calcd for $C_{26}Cl_2OP_2Ir$: C: 47.8; Cl: 10.9; O: 2.4; P: 9.5; Ir: 29.4. Found: C: 47.4; Cl: 6.7; O: 4.3; P: 12.2; Ir: 29.4.

Synthesis of 8. At −30 °C a solution of 0.056 g (0.069 mmol) of **4** in 5 mL of THF is added to 0.019 g (0.066 mmol) of η^6-*p*-xylene molybdenum tricarbonyl. After 30 min the solution is cloudy and orange-brown. All volatiles are removed in vacuo, yielding the orange-brown bimetallic product **8**. Yield: 0.056 g (0.056 mmol; 84.8%). ^{1}H NMR (250.13 MHz, acetone-d_6): δ −17.30 (t, $^2J_{PH}$ = 12.56 Hz, 1H, IrH), 1.39 ($A_9XX'A_9'$, N = |$^3J_{PH}$ + $^5J_{PH}$| = 14.62 Hz, 18H, C(CH_3)$_3$), 1.57 ($A_9XX'A_9'$, N = |$^3J_{PH}$ + $^5J_{PH}$| = 14.62 Hz, 18H, C(CH_3)$_3$), 4.44 ([ABX]$_2$, J_{AB} = $^2J_{HH}$ = 16.90 Hz, N = |$^2J_{PH}$ + $^4J_{PH}$| = 10.96 Hz, 2H, CH_aH$_b$P), 4.80 ([ABX]$_2$, J_{AB} = $^2J_{HH}$ = 16.90 Hz, N = |$^2J_{PH}$ + $^4J_{PH}$| = 7.77 Hz, 2H, CH$_a$$H_b$P), 6.43 (m, 2H, =CH), 6.50 (m, 2H, =CH). ^{31}P{^{1}H} NMR (101.26 MHz, acetone-d_6): δ 48.3 (s). ^{19}F NMR (235.33 MHz, acetone-d_6): δ −78.0 (s, br). ^{13}C{^{1}H} NMR (62.90 MHz, acetone-d_6): δ 29.0 (s, br, C(*C*H$_3$)$_3$), 30.5 (s, br, C(*C*H$_3$)$_3$), 38.9 (AXX′, N = |$^1J_{PC}$ + $^3J_{PC}$| = 28.97 Hz, *C*(CH$_3$)$_3$), 39.9 (AXX′, N = |$^1J_{PC}$ + $^3J_{PC}$| = 22.23 Hz, *C*(CH$_3$)$_3$), 44.6 ([AX]$_2$, N = |$^1J_{PC}$ + $^3J_{PC}$| = 25.60 Hz, CH_2P), 95.1 ([AX]$_2$, N = |$^3J_{PC}$ + $^4J_{PC}$| + |$^4J_{PC}$ + $^5J_{PC}$| = 10.78 Hz, =CH), 100.3 (s, =CH), 127.8 (q, $^1J_{CF}$ = 51.65 Hz, CF_3), 129.0 (t, $^2J_{PC}$ = 8.42 Hz, C$^+$−Ir), 135.0 (s, CH*C*CH$_2$P), 175.3 (t, $^2J_{PC}$ = 7.41 Hz, Ir(CO)), 212.5 (s, Mo(CO)). IR (cm^{-1}, pellet on KBr): 2045 (vs), 2030 (vs), 1981 (vs), 1940 (s) ν(C=O). MS (FAB): *m/z* 843.2 [M$^+$ − OTf$^-$], calcd for $C_{29}H_{45}ClO_4P_2IrMo$: 843.2; 786.9 [M$^+$ − OTf$^-$ − 2CO], calcd for $C_{27}H_{45}ClO_2P_2IrMo$: 787.2; 759.1 [M$^+$ − OTf$^-$ − 3CO], calcd for $C_{26}H_{45}ClOP_2IrMo$: 759.2; 627.1 [M$^+$ − (OTf$^-$ + Mo(CO)$_3$ + H + Cl], calcd for $C_{26}H_{44}OP_2Ir$: 626.8. MS (FD): *m/z* 626.1 [M$^+$ − (OTf$^-$ + Mo(CO)$_3$ + 2H + Cl)], calcd for $C_{26}H_{43}OP_2Ir$: 625.8. EDX (weight fraction): Anal. Calcd for $C_{30}ClF_3O_7P_2SIrMo$: C: 38.1; Cl: 3.7; O: 11.8; P: 6.5; Mo + S: 13.5; Ir: 20.3. Found: C: 39.5; Cl: 2.9; O: 10.2; P: 10.8; Mo + S: 13.3; Ir: 19.2.

Computational Details. The structures of all complexes were optimized using the local density approximation SVWN[36,37] as well as the gradient-corrected B3LYP[38] hybrid functional. For this purpose the pseudo potential LACVP* basis set[39] was applied using the program Jaguar 4.1.[40] In the case of the charged compounds **4**, **7**, and **8** the anion has been omitted in the calculations (marked by primes). The relative energetic stabilities of the various complexes were obtained as follows: The total energy of **1** was set to 0 kcal/mol, and the energy differences of **4′/7′** (same structure but different counterions), **5**, **6**, and **8′** relative to **1** were derived according to the equations

$$E(\mathbf{4'/7'}) = E(\mathbf{1}) - E(\mathrm{H^-}) \quad \text{(i)}$$

$$E(\mathbf{5}) = E(\mathbf{1}) - E(\mathrm{H_2}) \quad \text{(ii)}$$

$$E(\mathbf{6}) = E(\mathbf{1}) - E(\mathrm{H_2}) - E(\mathrm{HCl}) \quad \text{(iii)}$$

$$E(\mathbf{8'}) = E(\mathbf{1}) - E(\mathrm{H^-}) + E(\mathrm{Mo(CO)_3}) \quad \text{(iv)}$$

Zero-point energy (ZPE) corrections were not included in these calculations because, with respect to the computational effort, frequency calculations could not be performed.

X-ray Crystal Structure Analysis of 4. An orange crystal measuring approximately 0.2 × 0.2 × 0.2 mm was grown by slow evaporation of the solvent from **4** in dichloromethane. X-ray diffraction data were collected using a Siemens P4 four-circle diffractometer operating at 173 K in the ω-scan mode. Details of data collection and structure refinement are summarized in Table 4. Measured intensities were corrected for Lorentz and polarization effects, and an empirical absorption correction using φ-scans was applied. Structure solution and refinement was carried out with the Bruker XShell 4.01 suite of programs, incorporating SHELXS-97[41] for structure solution and SHELXL-97[42] for structure refinement. The structure was solved by direct methods, and most of the non-hydrogen atoms were located in the initial electron density map and the rest of them in subsequent difference Fourier maps. All hydrogen atoms were geometrically placed and allowed to ride on the atom to which they are connected.

Table 4. Crystal Data and Structure Refinement for 4

formula	$C_{28}H_{46}Cl_3F_3IrO_4P_2S$
M [g mol^{-1}]	896.20
space group	$P\bar{1}$
a [Å]	9.1124(15)
b [Å]	14.864(5)
c [Å]	15.610(2)
α [deg]	62.273(18)
β [deg]	87.045(13)
γ [deg]	76.072(16)
V [Å^3]	1812.0(7)
Z	2
ρ_{calcd} [g cm^{-3}]	1.643
radiation	Mo Kα (λ = 0.71073 Å)
μ [mm^{-1}]	4.097
θ range for data collection (deg)	2.31 to 27.50
index ranges	$-11 \le h \le 1$; $-16 \le k \le 16$; $-20 \le l \le 20$
no. of reflns collected	15 714
no. of unique reflns	7877
refinement method	full-matrix least-squares on F^2
no. of params	392
GoF on F^2	1.082
wR2[a]	0.0887 (obsd data); 0.0924 (all data)
R1[b]	0.0375 (obsd data); 0.0465 (all data)
final difference Fourier map [e Å^{-3}]	max: 4.251; min: −1.776

[a] $wR2 = [\sum[w(F_o^2 - F_c^2)^2]/\sum[wF_o^2)^2]]^{0.5}$; $w = [\exp(5\sin\theta)^2]/[\sigma^2(F_o^2) + 6.3966P + (0.039P)^2]$; $P = [F_o^2 + 2F_c^2]/3$. [b] $R1 = \sum(||F_o| - |F_c||)/\sum|F_o|$.

Acknowledgment. We thank the Fonds der Chemischen Industrie for financial support. A.M.W. gratefully acknowledges the DAAD and the Studienstiftung des Deutschen Volkes for a scholarship. W.C.K. thanks the National Science Foundation for support of this research. We are also grateful to Prof. Dr. E. Plies and Dr. S. Steinbrecher for the EDX measrements.

Supporting Information Available: Tables of crystal data, collection and refinement data, atomic coordinates, bond distances and angles as well as anisotropic displacment coefficients for complex **4**. Atomic coordinates of the optimized structures for complexes **1**, **4′/7′**, **5**, **6**, and **8′**. This material is available free of charge via the Internet at http://pubs.acs.org.

OM049289+

(36) Slater, J. C. *Quantum Theory of Molecules and Solids*; McGraw-Hill: New York, 1974.
(37) Vosko, S. H.; Wilk, L.; Nusair, M. *Can. J. Phys.* **1980**, *58*, 1200.
(38) Becke, A. D. *J. Chem. Phys.* **1993**, *98*, 5648.
(39) Hay, P. J.; Wadt, W. R. *J. Chem. Phys.* **1985**, *82*, 299.
(40) *Jaguar* (4.1); Schrödinger, Inc.: Portland, OR, 1991.
(41) Sheldrick, G. M. *Acta Crystallogr.* **1990**, *A46*, 467.
(42) Sheldrick, G. M. *SHELXL-97*, Program for the Refinement of Crystal Structures; University of Göttingen: Germany, 1997.